Optical Addressing of Pulses in a Semiconductor-Based Figure-of-Eight Fiber Laser

D. Chaparro[1] and Salvador Balle[1,2]
[1]Departamento de Física, Universitat de les Illes Balears, Carretera de Valldemossa, km 7.5, E-07122 Palma de Mallorca, Spain
[2]Institut Mediterrani d'Estudis Avançats, IMEDEA (CSIC-UIB), Carrer de Miquel Marqués 21, E-07190 Esporles, Spain

(Received 7 June 2017; revised manuscript received 29 August 2017; published 8 February 2018)

We experimentally demonstrate that optical pulses emitted by a semiconductor-based polarization-maintaining figure-of-eight fiber laser are temporal localized structures that can be individually switched on and off by means of optical reinjection of single pulses at different delay times. We also explore the formation of an equispaced cluster of localized structures that can be interpreted as a portion of an underlying periodic pattern—the harmonic state—and we provide a basic theoretical scenario for explaining the observations.

DOI: 10.1103/PhysRevLett.120.064101

Localized structures (LSs) are states characterized by a correlation range much shorter than the characteristic size of the system, appearing in many nonlinear dissipative systems [1]. The concept of LSs originated in the field of pattern formation for describing the inhomogeneous spatial distribution of some order parameter, and it represents one of the paradigms of self-organization. Spatial LSs arise in systems like granular media [2], gas discharges [3], semiconductor devices [4], reaction-diffusion systems [5], fluids [6], convective systems [7], optical cavities [8,9], etc. LSs may arise when different states coexist—the most common case being that of the coexistence of a homogeneous and a modulated state whose period is much shorter than the size of the system, hereby ensuring a large enough aspect ratio—although more complex scenarios can be found; see Refs. [10,11] for a review. In the most common scenario, LSs are interpreted as the elementary constituents of the modulated state. Their coexistence with a homogeneous state makes LSs individually addressable objects which can be created or destroyed independently without disturbing the rest of the system; hence, they can be used as bits for information processing and storage. While the precise theoretical definition of LSs is still under debate [12], an operational definition based on their addressability is usually adopted [13–15].

Recently, the concept of LSs has been extended to the time domain [16–19], particularly for optical resonators [20]. Temporal LS (TLSs) appear as short optical pulses, although we should remark that not all pulse-emitting devices produce TLS since these pulses may be highly correlated in time—this is the case for most mode-locked lasers [12]. TLS are observed, e.g., in injected fiber resonators [16], passively mode-locked lasers [13–15,21], and single mode vertical-cavity surface-emitting lasers (VCSELs) [22]. In optical systems, TLSs allow us to achieve extremely high peak irradiances that enable the exploration of extreme nonlinear optical effects in matter. Several interesting regimes (e.g., soliton bound states [23], molecules [24], repulsive or attracting forces on an extremely long scale [25], soliton rain [26], and soliton explosion [27]) have been experimentally observed.

TLSs may yield short optical pulses with arbitrary pulse arrangements useful in such fields as telecommunications, metrology, remote sensing, and material processing. For these applications, controlling the number and arrangement of the pulses is of the utmost importance. Léo *et al.* [16] demonstrated that optical injection in a passive fiber resonator can be used for defining the pulse pattern. In active systems, Refs. [15,21] showed that TLSs emitted by a VCSEL with an intracavity saturable absorber can be written, erased, and manipulated in position through control of the bias current applied to the laser, although this method is more limited in accuracy, flexibility, and speed than optical injection.

In this Letter, we focus on the optical addressing of the pulses emitted by the so-called figure-of-eight lasers (F8Ls). From the application point of view, optical injection allows us to optically perturb the system at any specific times without the speed limits imposed by the electronics of the device, thereby overcoming certain limitations of Refs. [15,21]. F8Ls involve two fiber loops, with one being unidirectional. The coupler connecting the loops acts as a nonlinear optical switch, whose transmittivity depends on the nonlinear phase shift acquired by the optical fields upon passing through an amplifying medium [28]. In our case, the gain medium is a fiber-coupled semiconductor optical amplifier (SOA) [29–31], and all of the fibers and components in the F8L system are polarization maintaining (PM) to avoid nonlinear polarization evolution in the cavity due to thermal and mechanical fluctuations. This kind of F8L produced trains of optical pulses 247 fs wide at repetition frequencies ranging from 18 MHz (inverse of the round-trip time) up to a harmonic state with a repetition rate of 2.5 GHz [32]. Compared to the systems in Refs. [14,21], the F8L is

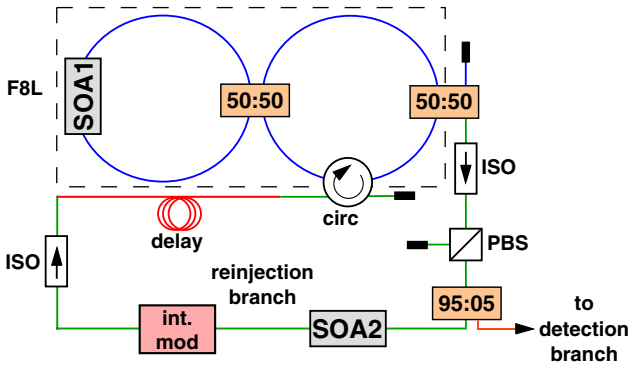

FIG. 1. Schematics of the F8L setup. SOA: semiconductor optical amplifier. circ: circulator. ISO: optical isolator. PBS: polarization beam splitter. Int. mod: intensity modulator. See the text for a detailed description.

lightweight, compact, and fiber integrated—ensuring low loss, good mode quality, and mechanical stability. Here, we experimentally demonstrate that, through optical reinjection of single pulses into the original pulse train at different delay times, we are able to individually switch on additional pulses in the system without perturbing the rest of the system. We observe that there are preferred delays where the written pulses remain for a very long time after reinjection removal, and we profit from these to demonstrate that the pulses can be switched off by optical injection. Moreover, the original pulses can be extinguished by the proper choice of a delay time, so pulses from the F8L can be interpreted as TLSs within one round-trip time. Finally, we explore the formation of clusters of equally spaced LSs interpreted as portions of the periodic underlying pattern (the harmonic state), and we discuss a basic theoretical model for explaining the observations.

The setup of the F8L (see Fig. 1) is similar to that used in Ref. [32], suitably modified to allow optical injection into the cavity. The F8L is defined by two PM fiber loops coupled through a 50:50 PM fiber coupler. One loop (length ≈6 m) is purely passive, operating unidirectionally due to a PM four-port optical circulator that works in the $1 \rightarrow 2 \rightarrow 3 \rightarrow 4 \rightarrow 1$ scheme; hence, port 4 can be used to inject optical signals into the system. The other loop (length ≈5 m) includes a single-transverse mode PM fiber-coupled SOA (SOA1, Thorlabs BOA1004P) that provides the gain. Hence, our F8L has a total transit time of ∼55 ns and works as the so-called nonlinear amplifying loop mirror. The laser output from the 50:50 coupler in the unidirectional loop passes through a PM optical isolator and is split in two with a 95:5 PM fiber coupler. The beam containing 5% of the output power is used for detection (see Ref. [32] for a description of the detection branch), while the other beam is used for optical reinjection into the F8L cavity. The reinjection beam is amplified by a second SOA (SOA2), nominally identical to SOA1. A single pulse of the laser output is selected by a PM intensity modulator (Photline MX-LN-10) controlled with an electrical pulse generator (EPG) (Stanford Research Systems DG535) triggered by the sync signal of the oscilloscope. Adjusting the delay of the EPG with respect to the sync signal from the scope allows us to pick a single optical pulse; simultaneously, the current of SOA2 is externally gated to control the power of the reinjected pulse. The length of the reinjection branch determines the time delay of the reinjected pulse with respect to the pulse train (modulo the round-trip time). It can be changed by inserting PM fiber patch cords of different lengths; in our case, the minimum delay (no patch cord inserted) is 5 ns, and each meter of patch cord adds ∼5 ns to the delay. It is also possible to write pulses "below" the default of 5 ns by using a long enough fiber cord which imposes a total delay that exceeds the round-trip.

When the reinjection loop is not active, the F8L behaves similarly to that presented in Ref. [32], although the laser threshold is now higher due to the use of a 50:50 coupler ($I = I_{\mathrm{th}} \simeq 135$ mA for a substrate temperature of 20 °C). Close to threshold, the F8L emits light with a rather broad spectrum centered at the wavelength $\lambda \simeq 1575$ nm. In this regime, the light-current characteristics of the F8L exhibits a slight hysteresis, and it does not switch off until the bias current is reduced below 100 mA. In the time domain, the laser output exhibits a regular train of short pulses with a period of ≈55 ns (see the blue traces in Fig. 2) corresponding to the round-trip time in the fiber loops defining the F8L. The intensity autocorrelation measurement reveals that the shape of these pulses is still hyperbolic secant squared, being now much longer (1.35 ps FWHM) than those in Ref. [32] due to the substantially higher losses.

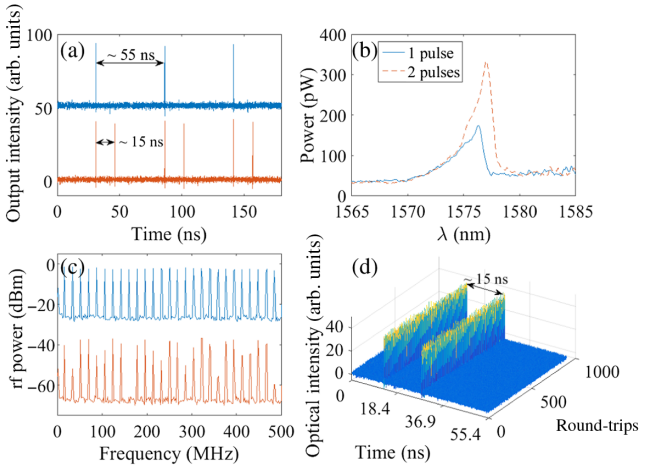

FIG. 2. (a) (Top) Time trace (blue) showing a single pulse per round-trip with a fundamental period of 55 ns at $I = 150$ mA (trace displaced upwards by 50 units for clarity). (Bottom) Pulse train (orange) with two pulses per round-trip (the second pulse is 15 ns from the first). (b) Optical spectrum of the traces in (a) where the solid line (blue) stays for the case of one pulse per round-trip and the dashed line (orange) for two pulses per round-trip. (c) (Top) rf spectrum of the fundamental state. (Bottom) State with two pulses per round-trip (the bottom spectrum is displaced downwards by 40 units for clarity). (d) Space-time diagram showing the stability of the two-pulse state over ∼1000 round-trips.

The rf spectrum displays a sharp peak at the fundamental frequency of 18 MHz, and a flat comb of replicas of this peak within the 5 GHz bandwidth of our rf amplifier. Increasing the bias current leads to a harmonic state with a regular pulse spacing, as in Ref. [32]. In the present case, however, the transition to the harmonic state does not occur gradually through the appearance of new pulses in the pulse train; instead, it occurs suddenly due to the increased cavity losses. Yet, multiple states presenting different number of pulses within a round-trip time organized with different time arrangements can still be observed by decreasing the bias current from the harmonic state (see Fig. 2). These states are stable (remaining for minutes or even longer), several of them coexist for the same value of the bias current, and the observed pulse shape is the same in all of them.

The coexistence of different states of the pulse train with a constant pulse shape but different pulse number and arrangements, together with the eventual development of a harmonic state, suggests that these pulses could be TLSs [15]. To verify this hypothesis, we set the F8L in its fundamental regime and proceed to activate the reinjection loop with a patch cord of 2.4 m, imposing a delay of 17 ns. Upon gating SOA2, a new pulse appears in the pulse train, which now displays two pulses per round-trip with a pulse separation of 17 ns. This new pulse train remains stable with that pulse separation as long as the bias current of SOA2 is not completely turned off. If the bias current of SOA2 is set to 0 mA, after a few seconds the pulse moves and places itself at ∼15 ns with respect to the reference pulse (see Fig. 3), where it remains fixed and stable for hours. A similar situation occurs when the reinjection is performed using a 6 m long fiber cord in the reinjection loop corresponding to a delay of 35 ns. Again, the pulse remains in this location while SOA2 is driven by some current, but it moves—in this case to 30 ns—after SOA2's current is turned off, remaining there for hours. These preferred pulse positions arise from the residual reflectivity of the connectors at the end of the 1.5 m long SOA pigtails: these imperfections in the setup pin the LSs to specific positions in the round-trip, similar to what happens in broad-area VCSELs, where imperfections in the mirrors defining the cavity pinned the LSs to specific positions in the transverse plane [33].

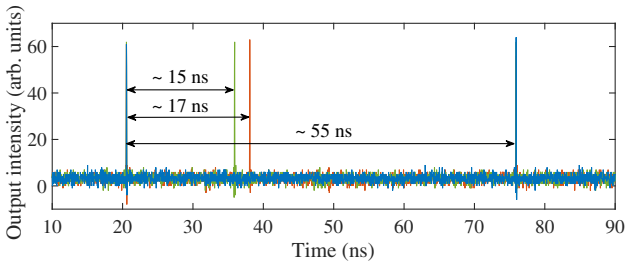

FIG. 3. A blue time trace of the fundamental state ($I = 150$ mA) indicating a pulsing period of 55 ns. The orange time trace was recorded after the injection of a second pulse with a delay of 17 ns (bias current in SOA2, $I_r = 80$ mA). The green time trace was recorded after injection of a second pulse with a delay of 17 ns (bias current in SOA2, $I_r = 0$ mA). The second pulse now appears with a delay of ∼15 ns.

To test the optical addressability of these pulses, a situation with pulses remaining for a very long time on their positions is required. We exploit these preferred positions using a 2 m long fiber cord in the reinjection arm (delay, ∼15 ns). By activating the reinjection arm in the fundamental state, a new pulse of the same shape is created at the corresponding delay time, remaining there indefinitely after the bias current of SOA2 is turned off [see Fig. 4(b)]. This new state with two pulses per round-trip at 15 ns is the same shown in greater detail in Fig. 2. In this state, by changing the delay of the EPG with respect to the sync signal in order to pick the second pulse of the pulse train, the activation of the reinjection arm leads to a state with three pulses per round-trip [Fig. 4(c)]. It is also possible to switch off an existing pulse by reinjecting another optical pulse on top of (or at least very close to) it, induced by gain depletion in the semiconductor (see the Supplemental Material [34]). If the delay between the EPG and the sync signal is now set for picking the fundamental pulse, this pulse is reinjected onto the second pulse and switched off, leading to a pulse train with two pulses per round-trip with a delay of 30 ns, as shown in Fig. 4(d). Instead, if the delay between the EPG and the sync signal is set for picking the second pulse, this pulse is reinjected into the third pulse of the signal and switched off, hereby recovering the pulse train with two pulses per round-trip with a delay of 15 ns, as shown in Fig. 4(e). The same process can also be performed by changing the length of the

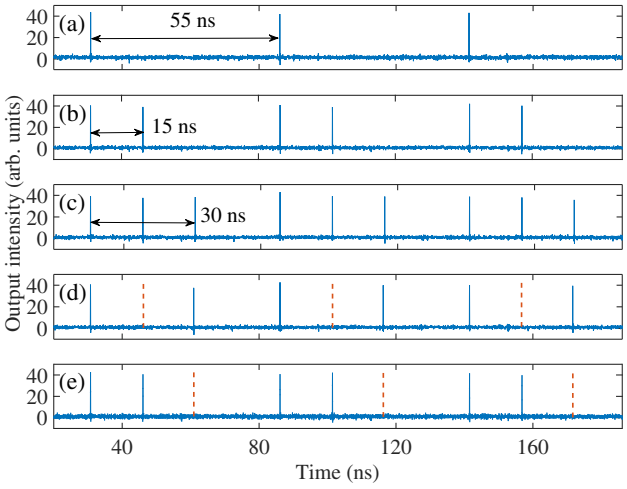

FIG. 4. Time traces showing the optical addressing of pulses with a reinjection delay of ∼15 ns. (a) Fundamental state with pulses at ∼55 ns. (b) State with two pulses per period obtained by reinjection of a pulse. (c) State with three pulses per period obtained by reinjection of the second pulse in (b). (d) State with two pulses per period with a spacing of 30 ns obtained from (c) by reinjection of the first pulse in (c). (e) State (b) recovered from (c) by reinjection of the second pulse.

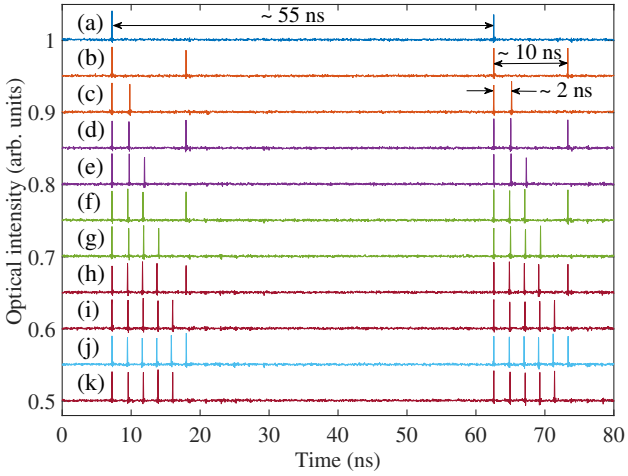

FIG. 5. Creation of a cluster of pulses with spacing ∼2 ns. (a) Fundamental state. (b) Reinjection of the first pulse in (a) at 10 ns. (c) Displacement of the second pulse in (b) at 2 ns from the first pulse when the reinjection current is turned off. From (d)–(j), iterative procedure of the previous steps to create a six pulse cluster. (k) Erasure of the sixth pulse of the package by reinjecting on top of it. See the text for explanation.

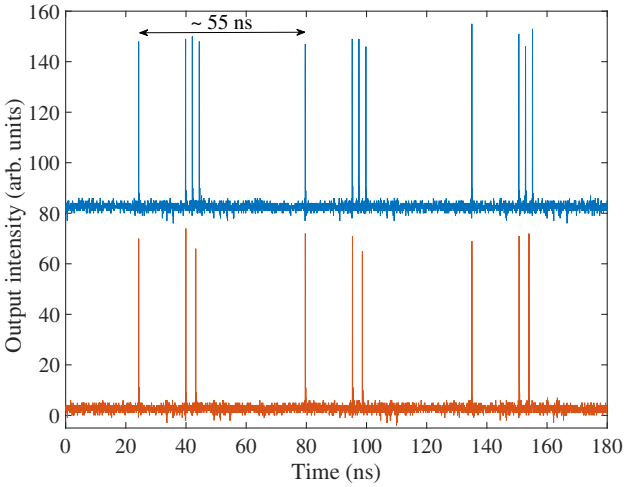

FIG. 6. Erasure of the central pulse of a three-pulse cluster.

fiber patch cord instead of modifying the delay in the EPG, indicating that the interaction of the optical reinjection with the pulse train is not phase sensitive but instead mediated by the active material.

For reinjection at ∼10 ns (see Fig. 5), the new pulse remains in its position for shorter times (tens of seconds) after the bias current in the SOA2 is set to zero. This pulse usually jumps to the preferred position at 15 ns or—most often—moves to the proximity of the preceding pulse (at ∼2 ns), where it remains to form a bound state of two pulses [see Fig. 5(c)]. Activating again the reinjection loop without modifying its settings allows us to write a new pulse in the train 10 ns from the first one. Interestingly, a short time after the SOA2 current drops to zero, the new pulse jumps to the vicinity of the bound state, placing itself at ∼2 ns from the second pulse in the bound state and leading to a three-pulse bound state [Fig. 5(e)]. The procedure can be repeated until forming a bound state of six pulses with 2 ns pulse spacing, which we interpret as a portion of the modulated state that coexists with the homogeneous off solution [10,11]. At this stage, the sixth pulse lays precisely 10 ns from the first pulse in the bound state [Fig. 5(j)], and activating the reinjection arm again without modifying its settings leads to switching off this sixth pulse [Fig. 5(k)]. Hence, although bounded, the sixth pulse still preserves its properties as a TLS since it can be switched on or off at will without affecting the rest of the bound state. The pulses in the middle of the cluster also retain their character as TLSs (see Fig. 6). The upper trace displays a cluster of three pulses with a delay of ∼15 ns respect to the fundamental pulse, and an almost regular spacing of ∼2 ns between pulses in the cluster. In this state, reinjection of the fundamental pulse with a fiber patch cord 2.5 m long (delay, ∼17.5 ns) allows us to switch off the central pulse of the cluster (see the bottom trace). As a consequence of the reduction in intracavity power, the timing of the third pulse slightly changes, passing from 20 to 19 ns.

A basic theoretical understanding of the pulsing dynamics of a F8L can be achieved with the model presented in the Supplemental Material [34]. In the fundamental pulsing regime, the single pulse in the unidirectional loop is split in two at the 50:50 coupler. These two counterpropagating pulses arrive at different times into the SOA1, which is periodically subject to the nonsimultaneous saturation imposed by these two pulses. The dynamics of the system can then be described by an iterative map, whose solution allows us to reconstruct the spatiotemporal distribution of the local gain (see the Supplemental Material [34]).

Summarizing, we have studied the optical reinjection of pulses into a polarization-maintaining figure-of-eight laser which has a SOA as its gain medium. The coexistence of multiple lasing states from the F8L under the same parameters and the independent writing and erasing of optical pulses indicate that they can be interpreted as TLSs. These TLSs can be placed at any position within the round-trip and remain there when the bias current of the SOA2 is not zero. Turning the bias current off reveals preferred positions for the LS towards which they displace. Furthermore, interactions between LSs lead to the formation of bound states of several pulses, retaining their individuality. These features can be useful for generating periodic trains with arbitrary pulse patterns.

We acknowledge the useful discussions with and comments from Professor M. Sorel (University of Glasgow) and Dr. L. Furfaro (University of Franche-Comté), and the financial support from Plan Estatal de Investigación Científica y Técnica y de Innovación, Ministerio de Economía y Competitividad (Spain) through Project No. TEC2015-65212-C3-3-P.

[1] M. Tlidi, K. Staliunas, K. Panajotov, A. G. Vladimirov, and M. G. Clerc, Phil. Trans. R. Soc. A **372**, 20140101 (2014).

[2] P. B. Umbanhowar, F. Melo, and H. L. Swinney, Nature (London) **382**, 793 (1996).

[3] Yu. A. Astrov and H.-G. Purwins, Phys. Lett. A **283**, 349 (2001).

[4] F.-J. Niedernostheide, M. Arps, R. Dohmen, H. Willebrand, and H.-G. Purwins, Phys. Status Solidi B **172**, 249 (1992).

[5] K.-J. Lee, W. D. McCormick, J. Pearson, and H. L. Swinney, Nature (London) **369**, 215 (1994).

[6] J. Wu, R. Keolian, and I. Rudnick, Phys. Rev. Lett. **52**, 1421 (1984).

[7] E. Moses, J. Fineberg, and V. Steinberg, Phys. Rev. A **35**, 2757 (1987).

[8] L. A. Lugiato, Chaos Solitons Fractals **4**, 1251 (1994).

[9] L. A. Lugiato, IEEE J. Quantum Electron. **39**, 193 (2003).

[10] P. Coullet, C. Riera, and C. Tresser, Phys. Rev. Lett. **84**, 3069 (2000).

[11] P. Mandel and M. Tlidi, J. Opt. B **6**, R60 (2004).

[12] N. N. Rosanov, S. V. Fedorov, and A. N. Shatsev, in *Dissipative Solitons: From Optics to Biology and Medicine*, edited by N. Akhmediev and A. Ankiewicz (Springer, New York, 2008), p. 93.

[13] P. Grelu and N. Akhmediev, Nat. Photonics **6**, 84 (2012).

[14] M. Marconi, J. Javaloyes, S. Balle, and M. Giudici, Phys. Rev. Lett. **112**, 223901 (2014).

[15] M. Marconi, J. Javaloyes, P. Camelin, D. Chaparro González, S. Balle, and M. Giudici, IEEE J. Sel. Top. Quantum Electron. **21**, 1101210 (2015).

[16] F. Leo, S. Coen, P. Kockaert, S.-P. Gorza, P. Emplit, and M. Haelterman, Nat. Photonics **4**, 471 (2010).

[17] T. Herr, V. Brasch, J. D. Jost, C. Y. Wang, N. M. Kondratiev, M. L. Gorodetsky, and T. J. Kippenberg, Nat. Photonics **8**, 145 (2014).

[18] M. Tlidi and L. Gelens, Opt. Lett. **35**, 306 (2010).

[19] M. Tlidi, L. Bahloul, L. Cherbi, A. Hariz, and S. Coulibaly, Phys. Rev. A **88**, 035802 (2013).

[20] S. Barland, S. Coen, M. Erkintalo, M. Giudici, J. Javaloyes, and S. Murdoch, Adv. Phys. X **2**, 496 (2017).

[21] P. Camelin, J. Javaloyes, M. Marconi, and M. Giudici, Phys. Rev. A **94**, 063854 (2016).

[22] M. Marconi, J. Javaloyes, S. Barland, S. Balle, and M. Giudici, Nat. Photonics **9**, 450 (2015).

[23] D. Y. Tang, W. S. Man, H. Y. Tam, and P. D. Drummond, Phys. Rev. A **64**, 033814 (2001).

[24] P. Grelu and J. Soto-Crespo, in *Dissipative Solitons: From Optics to Biology and Medicine*, edited by N. Akhmediev and A. Ankiewicz (Springer, New York, 2008), p. 1.

[25] J. K. Jang, M. Erkintalo, S. G. Murdoch, and S. Coen, Nat. Photonics **7**, 657 (2013).

[26] S. Chouli and P. Grelu, Phys. Rev. A **81**, 063829 (2010).

[27] S. T. Cundiff, J. M. Soto-Crespo, and N. Akhmediev, Phys. Rev. Lett. **88**, 073903 (2002).

[28] I. N. Duling III, Opt. Lett. **16**, 539 (1991).

[29] R. J. Manning, A. E. Kelly, K. J. Blow, A. J. Poustie, and D. Nesset, Opt. Commun. **157**, 45 (1998).

[30] K. Vlachos, C. Bintjas, N. Pleros, and H. Avramopoulos, IEEE J. Sel. Top. Quantum Electron. **10**, 147 (2004).

[31] H.-R. Chen, K.-H. Lin, C.-Y. Tsai, H.-H. Wu, C.-H. Wu, C.-H. Chen, Y.-C. Chi, G.-R. Lin, and W.-F. Hsieh, Opt. Lett. **38**, 845 (2013).

[32] D. Chaparro, L. Furfaro, and S. Balle, Photonics Res. **5**, 37 (2017).

[33] S. Barland *et al.*, Nature (London) **419**, 699 (2002).

[34] See Supplemental Material at http://link.aps.org/supplemental/10.1103/PhysRevLett.120.064101, which includes Refs. [35–37], for further details on the theoretical modeling of the F8L and the mechanism causing the erasure of the pulses.

[35] C. Antonelli and A. Mecozzi, IEEE Photonics Technol. Lett. **25**, 2243 (2013).

[36] C. Antonelli, A. Mecozzi, Z. Hu, and M. Santagiustina, J. Lightwave Technol. **33**, 4367 (2015).

[37] M. Brambilla, L. A. Lugiato, and M. Stefani, Europhys. Lett. **34**, 109 (1996).